


# Improved visualization of the chorda tympani nerve using ultra-high-resolution computed tomography

Acta Radiologica Open  
10(11) 1–7  
© The Author(s) 2021  
Article reuse guidelines:  
[sagepub.com/journals-permissions](https://sagepub.com/journals-permissions)  
DOI: 10.1177/20584601211061444  
[journals.sagepub.com/home/arr](https://journals.sagepub.com/home/arr)  


Masahiro Fujiwara<sup>1</sup> , Yoshiyuki Watanabe<sup>2</sup>, Nobuo Kashiwagi<sup>3</sup> , Yumi Ohta<sup>4</sup> , Takashi Sato<sup>4</sup>, Megumi Nishigaki<sup>5</sup> and Noriyuki Tomiyama<sup>1</sup>

## Abstract

**Background:** Recognition of the anatomical course of the chorda tympani nerve (CTN) is important for preventing iatrogenic injuries during middle-ear surgery.

**Purpose:** This study aims to compare visualization of the CTN using two computed tomography (CT) methods: conventional high-resolution CT (C-HRCT) and ultra-high-resolution CT (U-HRCT).

**Materials and methods:** We performed a retrospective visual assessment of 59 CTNs in normal temporal bones of 54 consecutive patients who underwent both C-HRCT and U-HRCT. After dividing CTN into three anatomical segments (posterior canaliculus, tympanic segment, and anterior canaliculus), two neuroradiologists scored the visualizations on a four-point scale.

**Results:** On C-HRCT, the visual scores of the posterior canaliculus, tympanic segment, and anterior canaliculus were  $3.5 \pm 0.7$ ,  $1.6 \pm 0.6$ , and  $3.1 \pm 0.7$ , respectively. The respective values were significantly higher in all segments on U-HRCT:  $3.9 \pm 0.2$ ,  $2.4 \pm 0.6$ ,  $3.5 \pm 0.6$  ( $p < 0.01$ ). Although the difference in scores between methods was greatest for the tympanic segment, the visual score on U-HRCT was lower for the tympanic segment than for the anterior and posterior segments ( $p < 0.01$ ).

**Conclusion:** Ultra-high-resolution CT provides superior visualization of the CTN, especially the tympanic segment.

## Keywords

Chorda tympani nerve, ultra-high-resolution CT, surgical anatomy, temporal bone

Received 16 September 2021; Accepted 3 November 2021

## Introduction

The chorda tympani nerve (CTN) is a branch of the facial nerve. Its main function is to carry taste sensations from the anterior two-thirds of the tongue and to provide parasympathetic secretomotor innervation of the sublingual and submandibular glands<sup>1</sup>. Anatomically, the CTN is divided into three segments: the posterior canaliculus, the tympanic segment, and the anterior canaliculus. The nerve branches from the mastoid segment of

<sup>1</sup>Diagnostic and Interventional Radiology, Osaka University Graduate School of Medicine, Suita, Japan

<sup>2</sup>Department of Radiology, Shiga University of Medical Science, Otsu, Japan

<sup>3</sup>Future Diagnostic Radiology, Osaka University Graduate School of Medicine, Suita, Japan

<sup>4</sup>Otorhinolaryngology, Osaka University Graduate School of Medicine, Suita, Japan

<sup>5</sup>Canon Medical Systems, Otawara, Japan

### Corresponding author:

Masahiro Fujiwara, Diagnostic and Interventional Radiology, Osaka University Graduate School of Medicine, 2-2, Yamadaoka, Suita, Osaka 565-0871, Japan.

Email: [m-fujiwara@radiol.med.osaka-u.ac.jp](mailto:m-fujiwara@radiol.med.osaka-u.ac.jp)



Creative Commons Non Commercial CC BY-NC: This article is distributed under the terms of the Creative Commons Attribution-NonCommercial 4.0 License (<https://creativecommons.org/licenses/by-nc/4.0/>) which permits non-commercial use, reproduction and distribution of the work without further permission provided the original work is attributed as specified on the SAGE and Open Access pages (<https://us.sagepub.com/en-us/nam/open-access-at-sage>).

the facial nerve pass anterosuperiorly through the posterior canaliculus, cross the middle-ear cavity, and run through the anterior canaliculus after exiting the tympanum, which is within the medial part of the petrotympanic fissure.<sup>1–3</sup>

Chorda tympani nerve is often damaged during surgical procedures, especially in middle-ear surgery.<sup>4,5</sup> Its long course and limited preoperative visualization make it susceptible to iatrogenic injury.<sup>3,6</sup> Trauma to the temporal bone can also damage the CTN.<sup>7</sup> To prevent or evaluate these injuries, it is important to visualize the CTN using medical imaging. Conventional high-resolution computed tomography (C-HRCT) enables the visualization of the posterior and anterior canaliculi through multiplanar reconstruction. However, the tympanic segment of the CTN is not easily visualized because it runs through the air space of the tympanic cavity.<sup>2,3</sup>

Recent advances in imaging include ultrahigh-resolution CT (U-HRCT), which uses smaller detector elements and X-ray tubes with a smaller focal spot that can provide greater in-plane spatial resolution and thinner slice sections. U-HRCT can be used to provide a detailed delineation of lung structures and arteries supplying the spinal cord.<sup>8–11</sup> Therefore, we expected that U-HRCT would visualize the CTN more clearly than C-HRCT. The purpose of this study was to evaluate whether U-HRCT can provide better visualization of the CTN than C-HRCT.

## Material and methods

### Patients

This retrospective study was approved by the institutional review board, and the requirement to obtain informed consent was waived because of the retrospective design. We collected data of 450 patients who underwent U-HRCT of the temporal bone from January 2018 to December 2019 and selected eligible patients who had undergone C-HRCT of the temporal bone within 5 years. The exclusion criteria were a slice thickness > 0.625 mm on C-HRCT, bilateral temporal bone abnormalities, or a history of surgery. Finally, we enrolled a total of normal 59 temporal bones in 54 patients, who included 23 men and 31 women with an average age of 58 years (age range of 20–88 years).

### Image acquisition and reconstruction

Ultra-high-resolution CT was performed with a U-HRCT scanner (Aquilion Precision, Canon Medical Systems, Otawara, Japan). The scanning parameters were as follows: voltage, –120 kV; current, –200 mA; rotation speed, –1.0 s/rot; and super high-resolution scan mode. The images were reconstructed separately for the left and right sides using a

slice thickness of 0.25 mm at 0.25-mm intervals, a reconstruction field of view (FOV) of 120 mm, with a matrix size of 1024 × 1024, a voxel size of 0.12 × 0.12 × 0.25 mm, and a reconstruction kernel of FC80 (bone kernel).

High-resolution computed tomography was performed with several scanners: Aquilion ONE (Canon Medical Systems), Discovery CT 750HD (GE Healthcare, WI, USA), and LightSpeed VCT (GE Healthcare). The scanning parameters were as follows: voltage, –120 kV; current, –100 or 250 mA; slice thickness, –0.50 or 0.625 mm at 0.50 or 0.625 mm intervals; reconstruction FOV, –120 mm; matrix size, –512 × 512; voxel size, –0.23 × 0.23 × 0.50/0.625 mm; and bone kernel.

### Image evaluation

First, the CTN was divided into three segments: posterior canaliculus, tympanic segment, and anterior canaliculus. Second, two neuroradiologists (MF and NK with 6 and 26 years of experience in neuroradiology, respectively) independently evaluated each segment of the CTN by scoring its degree of visualization on a four-point scale (1 = not visible; 2 = partially visible; 3 = mostly visible, but partially invisible; 4 = entirely visible) on reconstructed axial images obtained from C-HRCT. The window level and width could be modified by the reviewers. The same evaluation was subsequently performed on the axial images of U-HRCT after an interval of at least 4 weeks to minimize recall bias. Since the difference between the images obtained from U-HRCT and C-HRCT was visually obvious, the two neuroradiologists were not blinded. In cases with discrepancies between the two readers, consensus was reached for the final score. To obtain the radiation dose, we extracted records of the volume CT dose index for each scan.

### Statistical analysis

The agreement between the two radiologists for the visualization scores was assessed using Cohen's kappa test. Differences in the visualization scores between C-HRCT and U-HRCT were assessed using the Wilcoxon matched-pairs signed rank test. Differences in the CT dose index between C-HRCT and U-HRCT were assessed using the paired t-test. A *p*-value < 0.01 was considered as significant. All analyses were performed using the R statistical software (R Core Team (2019). R: A language and environment for statistical computing. R Foundation for Statistical Computing, Vienna, Austria. URL <https://www.R-project.org/>).

## Results

The agreement between the two radiologists for the CTN visualization scores was good (Cohen's kappa = 0.79; weighted Cohen's kappa = 0.86). The mean visualization

**Table 1.** The mean visualization score for each segment of the chorda tympani nerve in high-resolution computed tomography and ultra-high-resolution computed tomography.

	Score (mean $\pm$ SD)		<i>p</i> value
	C-HRCT	U-HRCT	
Posterior canaliculus	3.5 $\pm$ 0.7	3.9 $\pm$ 0.2	< 0.001*
Tympanic segment	1.6 $\pm$ 0.6	2.4 $\pm$ 0.6	< 0.001*
Anterior canaliculus	3.1 $\pm$ 0.7	3.5 $\pm$ 0.6	< 0.001*

SD: standard deviation; C-HRCT: conventional high-resolution computed tomography; U-HRCT: ultra-high-resolution computed tomography.

scores for each segment of CTN on C-HRCT and U-HRCT are shown in Table 1. In all segments, the mean visualization scores were significantly higher on U-HRCT than on C-HRCT (all *p* values < 0.001). The respective visualization scores on U-HRCT and C-HRCT were 3.9  $\pm$  0.2 and 3.5  $\pm$  0.7 in the posterior canaliculus, 2.4  $\pm$  0.6 and 1.6  $\pm$  0.6 in the tympanic segment, and 3.1  $\pm$  0.7 and 3.5  $\pm$  0.6 in the anterior canaliculus.

The difference in the mean visualization scores between the two methods was greatest in the tympanic segment. However, the mean visualization score was significantly lower for the tympanic segment than for the posterior and anterior canaliculi in U-HRCT (*p* < 0.01). The distribution

of the visualization scores for each segment is shown in Figure 1 and Table 2. The score for the tympanic segment on C-HRCT changed from 1 to 2 in 20 subjects, from 1 to 3 in two, and from 1 to 4 in one subject. Images from a representative case that showed improved visualization of the CTN on U-HRCT are shown in Figure 2. The volume CT dose index did not significantly differ between the methods  $-45.7 \pm 11.8$  mGy for C-HRCT and  $46.3 \pm 2.0$  mGy for U-HRCT (*p* = 0.72).

## Discussion

Recently, several studies have evaluated the delineation ability of U-HRCT for normal structures of temporal bones,<sup>12–14</sup> and Hiraumi et al. have presented the tympanic segment of CTN using U-HRCT.<sup>14</sup> However, their study was performed only in 11 healthy volunteers and did not evaluate the entire course of the CTN. In contrast, our study evaluated the entire course of CTNs in a larger population including elderly patients, which seems to be meaningful.

Our data shows that the visualization score was significantly higher for U-HRCT than for C-HRCT in all segments of the CTN. This has been observed in previous studies that evaluated microstructures in other anatomical sites such as the lung or vessels feeding the spinal cord.<sup>8–11</sup> The higher in-plane spatial resolution and thinner slice

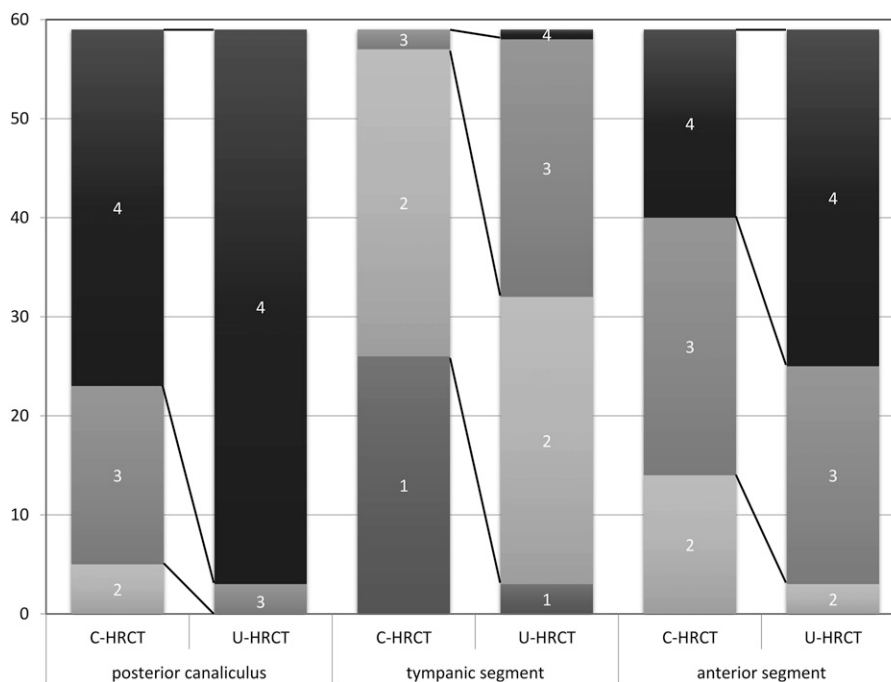


**Figure 1.** Distribution of visual scores for each segment of the chorda tympani nerve in C-HRCT and U-HRCT. The distribution of the visualization score was higher in the U-HRCT group for all segments, especially in the tympanic segment. The score for the tympanic segment on C-HRCT changed from 1 to 2 in 20 subjects, from 1 to 3 in two, and from 1 to 4 in one subject. C-HRCT: high-resolution computed tomography; U-HRCT: ultra-high-resolution computed tomography.

**Table 2.** Visualization score for each segment of the chorda tympani nerve on high-resolution computed tomography and ultra-high-resolution computed tomography.

Score	Posterior canaliculus		Tympanic segment		Anterior canaliculus	
	C-HRCT	U-HRCT	C-HRCT	U-HRCT	C-HRCT	U-HRCT
4	36	56	0	1	19	34
3	18	3	2	26	26	22
2	5	0	31	29	14	3
1	0	0	26	3	0	0

C-HRCT: conventional high-resolution computed tomography; U-HRCT: ultra-high-resolution computed tomography.

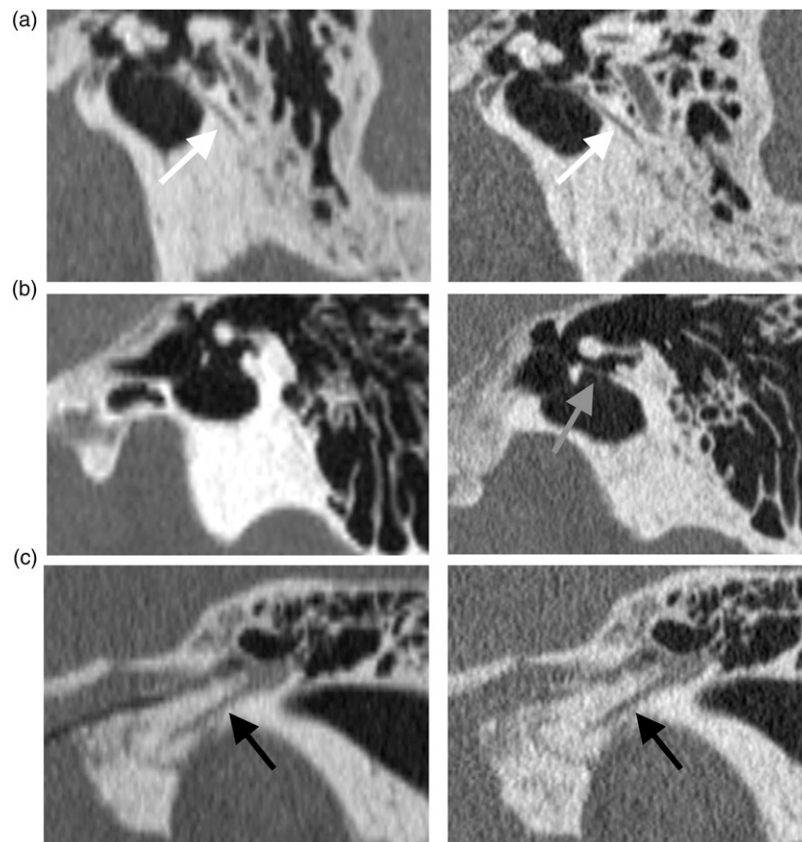


**Figure 2.** Comparison between C-HRCT and U-HRCT images of the chorda tympani nerve. Images of the left side (a) posterior canaliculus (white arrow), (b) tympanic segment (gray arrow), and (c) anterior canaliculus (black arrow) were obtained using C-HRCT, and those of the right side were obtained using U-HRCT. All segments are visualized more clearly on U-HRCT than on C-HRCT, especially in the tympanic segment. The tympanic segment cannot be seen on C-HRCT but can be seen on U-HRCT. C-HRCT: high-resolution computed tomography; U-HRCT: ultra-high-resolution computed tomography.

thickness provided by U-HRCT seem to enable a clearer boundary definition of all segments of the CTN.

Among the three segments of the CTN, the tympanic segment had the greatest increase in visualization score from C-HRCT to U-HRCT, which suggests that the main invisible tympanic segments on C-HRCT became partially visible on U-HRCT. This can be explained as follows. The tympanic segment of the CTN runs naked in

the air and has the lowest Hounsfield number of  $-1000$  HU. Therefore, the partial-volume effect conceals the visualization of the CTN because of the coexistence of nervous tissue and air. In addition, because of soft tissue, the tympanic segment of the CTN has inherently lower contrast compared to the anterior/posterior canaliculi, which are bony structures. Therefore, the thinner slice thickness and higher in-plane resolution provided by U-HRCT seem to

improve the visualization of the CTN most effectively in the tympanic segment.

Even with U-HRCT, the visual score of the CTN was still the lowest for the tympanic segment among the three segments. In addition to the abovementioned partial-volume effect, the following may explain this result further. The anterior mallear and discomalleolar ligaments in the tympanic cavity may affect visualization of the tympanic segment of the CTN. Anatomically, the tympanic segment can be subdivided before and after the gap between the malleus and

incus. Although both portions run in the air space of the tympanic cavity, after the gap, the CTN runs close to and parallel to the anterior mallear and discomalleolar ligaments.<sup>15-17</sup> Therefore, even with U-HRCT with its higher spatial resolution, distinguishing between the CTN and the anterior mallear and discomalleolar ligaments can be difficult (Figure 3).

Except for the well-known varied distances between the origin of the CTN from the facial nerve and the stylomastoid foramen,<sup>1-3</sup> there were no variations in the CTN when we

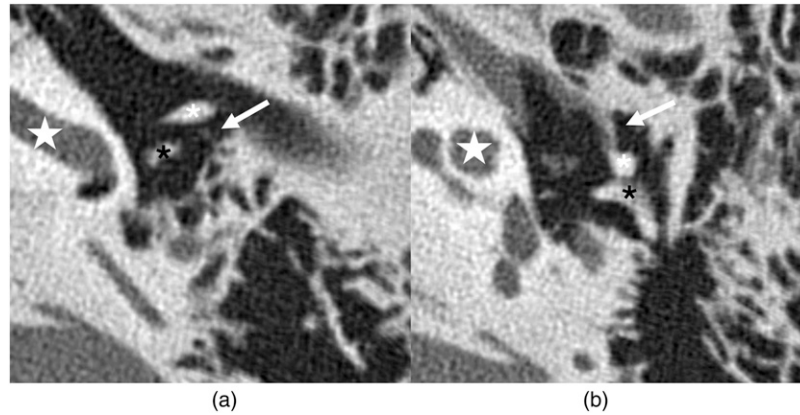


**Figure 3.** Difference in the visualization the tympanic segment of the CTN on ultra-high-resolution computed tomography between before and after the gap between the malleus and incus. (a) Before the gap between the malleus (white asterisk) and incus (black asterisk), the CTN is well visualized (arrow). (b) After the gap, it is difficult to identify the CTN because of the discomalleolar ligament and anterior malleolar ligament (arrow). The white star indicates the cochlea. CRN: chorda tympani nerve.

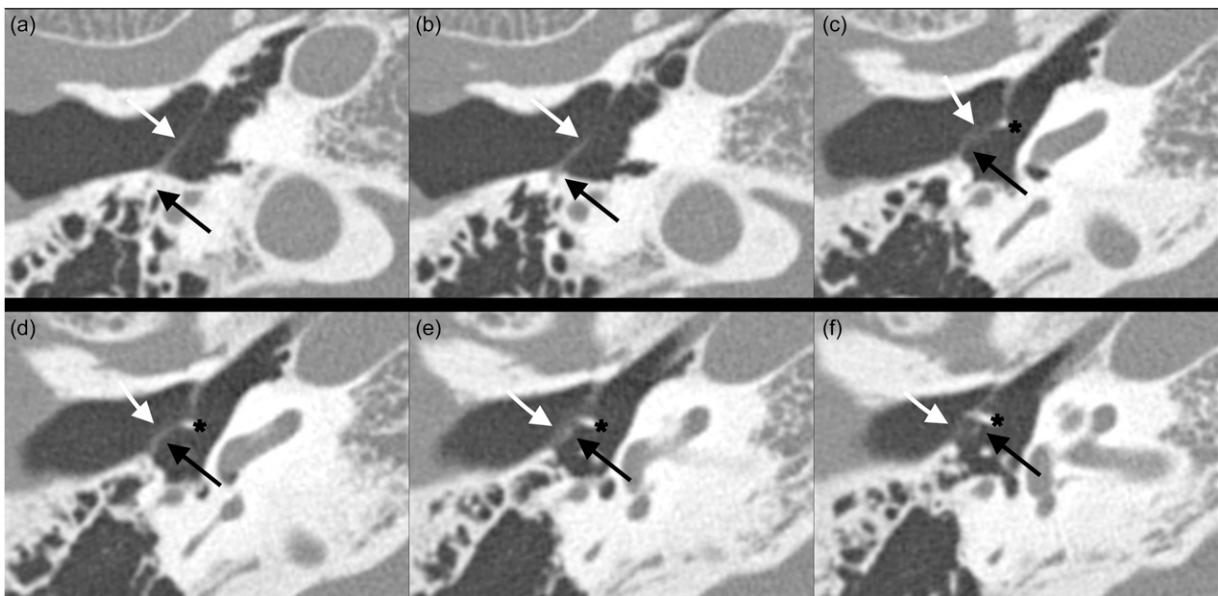


**Figure 4.** The CTN in contact with the tympanic membrane. Sequential axial ultra-high-resolution computed tomography images of the right temporal bone from bottom to top (a-f). The black arrow, white arrow, and black asterisk indicates the CTN, the tympanic membrane, and the malleus, respectively. The CTN runs through the posterior canalculus (a) and into tympanum (b). The CTN then runs in contact with the tympanic membrane, which appears to be thickened tympanic membrane (c and d). After that, the CTN separates from the tympanic membrane and travels to the malleus (e and f). CTN: chorda tympani nerve



evaluated the temporal bones. However, several CTNs were in contact with the tympanic membrane in their posterior tympanic segments, presumably as a post-inflammatory adhesion (Figure 4). In such cases, there might be a potential risk of damage to the CTN during invasive procedures, such as tympanostomy. Therefore, the improved visibility of the CTN on U-HRCT may have a clinical significance.

Our study has some limitations. First, since the sample size was small, we may not have included normal variants and could not check for differences according to age or sex. Further studies should include a larger sample size to examine these issues. Second, the scan dates were different for U-HRCT and C-HRCT, and it is possible that pathological changes or aging during the time lag may have influenced the results. However, the finding of superior visualization of the CTN using U-HRCT seems to be valid because all U-HRCT examinations were performed after the C-HRCT examinations in this study. Third, the image analysis could not be performed blindly because the difference between C-HRCT and U-HRCT was visually obvious; hence, our results might be biased by the subjective evaluations. Fourth, C-HRCT was performed using various CT scanners. The slice thickness obtained with these scanners differed (0.50 mm or 0.625 mm) as did the tube current (100 mA or 250 mA). Therefore, the image quality of C-HRCT might not have been homogenous.

In conclusion, the CTN can be visualized more clearly on U-HRCT than C-HRCT, especially in the tympanic segment.

### Declaration of conflicting interests

The author(s) declared no potential conflicts of interest with respect to the research, authorship, and/or publication of this article.

### Funding

The author(s) disclosed receipt of the following financial support for the research, authorship, and/or publication of this article: The co-author's chair (Y. Watanabe and N. Kashiwagi, Future Diagnostic Radiology Joint Research Chair, Graduate School of Faculty of Medicine, Osaka University) is funded by Canon Medical Systems. One co-author (M. Nishigaki) is an employee of Canon Medical Systems.

### Ethical approval

This retrospective study was approved by the institutional review board.

### Informed consent

This study was approved by the institutional review board, and written informed consent was waived because of the retrospective design.

### ORCID iDs

Masahiro Fujiwara  <https://orcid.org/0000-0003-3423-7658>

Nobuo Kashiwagi  <https://orcid.org/0000-0003-0986-6532>

Yumi Ohta  <https://orcid.org/0000-0002-5059-0876>

### References

- McManus L, Dawes P and Stringer M. Clinical anatomy of the chorda tympani: a systematic review. *J Laryngol Otol* 2011; 125: 1101–1108.
- McManus LJ, Dawes PJ and Stringer MD. Surgical anatomy of the chorda tympani: a micro-CT study. *Surg Radiol Anat* 2012; 34: 513–518.
- Singh D, Hsu CC-T, Kwan GNC, et al. High resolution CT study of the chorda tympani nerve and normal anatomical variation. *Jpn J Radiol* 2015; 33: 279–286.
- Kiverniti E and Watters G. Taste disturbance after mastoid surgery: immediate and long-term effects of chorda tympani nerve sacrifice. *J Laryngol Otol* 2012; 126: 34–37.
- McManus L, Stringer M and Dawes P. Iatrogenic injury of the chorda tympani: a systematic review. *J Laryngol Otol* 2012; 126: 8–14.
- Saito T, Manabe Y, Shibamori Y, et al. Long-term follow-up results of electrogustometry and subjective taste disorder after middle ear surgery. *Laryngoscope* 2001; 111: 2064–2070.
- Low HL and Redfern RM. Isolated chorda tympani injury following petrous temporal fracture. *J Clin Neurosci* 2008; 15: 716–718.
- Hata A, Yanagawa M, Honda O, et al. Effect of matrix size on the image quality of ultra-high-resolution CT of the lung: comparison of 512 × 512, 1024 × 1024, and 2048 × 2048. *Acad Radiol* 2018; 25: 869–876.
- Kakinuma R, Moriyama N, Muramatsu Y, et al. Ultra-high-resolution computed tomography of the lung: image quality of a prototype scanner. *PLoS One* 2015; 10: e0145357.
- Yoshioka K, Tanaka R, Takagi H, et al. Ultra-high-resolution CT angiography of the artery of Adamkiewicz: a feasibility study. *Neuroradiology* 2018; 60: 109–115.
- Yanagawa M, Hata A, Honda O, et al. Subjective and objective comparisons of image quality between ultra-high-resolution CT and conventional area detector CT in phantoms and cadaveric human lungs. *Eur Radiol* 2018; 28: 5060–5068.
- Yamashita K, Hiwatashi A, Togao O, et al. Ultrahigh-resolution CT scan of the temporal bone. *Eur Arch Otorhinolaryngol* 2018; 275: 2797–2803.
- Ohara A, Machida H, Shiga H, et al. Improved image quality of temporal bone CT with an ultrahigh-resolution CT scanner: clinical pilot studies. *Jpn J Radiol* 2020; 38: 878–883.
- Hiraumi H, Obara M, Yoshioka K, et al. Detectability of minute temporal bone structures with ultra-high resolution CT. *Auris Nasus Larynx* 2019; 46: 830–835.

15. Kim H, Jung H, Kwak H, et al. The discomalleolar ligament and the anterior ligament of malleus: an anatomic study in human adults and fetuses. *Surg Radiol Anat* 2004; 26: 39–45.
16. Ramírez Aristeguieta LM, Ballesteros Acuña LE and Sandoval Ortiz GP. A direct anatomical study of the morphology and functionality of disco-malleolar and anterior malleolar ligaments. *Int J Morphol* 2009; 27: 367–379.
17. Şencimen M, Yalçın B, Doğan N, et al. Anatomical and functional aspects of ligaments between the malleus and the temporomandibular joint. *Int J Oral Maxillofac Surg* 2008; 37: 943–947.